Wide-Band Microstrip-to-Coplanar Stripline/Slotline Transitions

Wen-Hua Tu, *Student Member, IEEE,* and Kai Chang, *Fellow, IEEE*

***Abstract*—Wide-band microstrip line to coplanar stripline (CPS) transitions are proposed. The transition consists of a multisection matching transformer and a quarter-wavelength radial stub for the impedance matching and field matching between the microstrip line and CPS, respectively. The proposed planar transition has the advantages of compact size, wide bandwidth, and straightforward design procedure. Several parameters are studied through simulations and experiments to derive some design guidelines. With the return loss of better than 14 dB, the 1- and 3-dB back-to-back insertion loss bandwidth can cover from 1.4 to 6.6 GHz (1 : 4.7) and from 1.1 to 10.5 GHz (1 : 9.6), respectively. In addition, the microstrip-to-CPS transition is extended to design a microstrip-to-slotline transition by tapering the CPS into a slotline. From 2.7 to 10.4 GHz (1 : 3.85), the back-to-back return loss is better than 15 dB and the insertion loss is less than 3 dB.**

***Index Terms*—Balun, coplanar stripline (CPS), slotline, transition.**

I. Introduction

THE COPLANAR stripline (CPS) is a balanced uniplanar transmission line with the advantages of compact size, ease of mounting lumped components in serious or shunt configuration, and low discontinuity parasitics. The uniplanar characteristics of the CPS also eliminate the need for a via-hole that introduces parasitic effects. Based on the above advantages, the CPS has found many applications in microwave circuits such as filters [1], mixers [2], phase shifters [3], and dipole antennas [4]. On the other hand, since the microstrip line is still one of the most popular transmission lines, the microstrip-to-CPS transition with wide bandwidth, low loss, and simple structure is required in order to fully take advantage of these two transmission lines.

Several microstrip-to-CPS transitions have been reported. The transition based on the mode conversion has shown a 3-dB back-to-back insertion loss bandwidth of 59% [5]. As an improved design of [5], a 3-dB back-to-back insertion loss bandwidth of 68% is achieved [6]. In addition, the transition using the coupling method shows a 2.4-dB back-to-back insertion loss bandwidth of 18% [7]. The above transitions, however, are only suitable for narrow-band applications. Furthermore, they are all built on high dielectric-constant substrates $(\varepsilon_r > 10)$ for a low characteristic impedance of the CPS, and easy matching to a 50-Ω microstrip line. Since the high dielectric-constant substrates are suitable for circuit design instead of the antenna design, using such transitions to feed antennas will degrade the antenna performance.

Recently, the microstrip-to-CPS transitions on low dielectric-constant substrates have been reported with a 3-dB back-to-back insertion loss bandwidth covering from 1.3 to 13.3 GHz (1 : 10.2) [8] and an 1-dB back-to-back insertion loss covering from 6.5 to 13.8 GHz [9]. However, these transitions use a long smooth tapered microstrip line and/or tapered ground plane to match the high characteristic impedance of CPS to the 50-Ω microstrip line and to obtain good field matching. The fabrication of the transitions requires accurate double-side etching and alignment. Furthermore, since there are no easy design equations for the long tapered lines or taper ground plane, the design of these transitions can only rely on time-consuming full-wave optimization.

In this paper, a wide-band microstrip-to-CPS transition based on coupling method is proposed. The proposed transition consists of a microstrip multisection matching transformer and a radial stub. Since there is no taper line or taper ground plane needed, the proposed transition is easy to fabricate. Furthermore, the taper ground causes more power loss that introduces crosstalk, which is undesired in high-density circuits. Based on the experimentally parametric studies and transmission-line equations, the design guidelines for the proposed transition are derived. The design guidelines can be used to obtain the initial dimensions for the full-wave optimization. Experiments have been carried out to verify the design concept with good agreement. With the return loss of better than 14 dB, the 1- and 3-dB back-to-back insertion loss bandwidth can cover from 1.4 to 6.6 GHz (1 : 4.7) and from 1.1 to 10.5 GHz (1 : 9.6), respectively. In addition, a wide-band microstrip line to slotline transition is investigated. The transition is consisted of a microstrip-to-CPS transition and a taper from CPS to slotline. From 2.7 to 10.4 GHz (1 : 3.85), the return loss is better than 15 dB and the insertion loss is better than 3 dB for a back-to-back transition. Although this paper only shows the transitions on low constant substrates for antenna applications, it should be mentioned that the design concept could also be used to design the transitions on high dielectric-constant substrates for circuit applications.

II. Microstrip-to-CPS Transition Design and Measurement

A. Impedance and Field Matching

Fig. 1 shows the configurations of the proposed transitions. To design a transition, a field matching and an impedance matching are required [10]. Since the electric field in the microstrip line

Manuscript received April 9, 2005.

The authors are with the Department of Electrical Engineering, Texas A&M University, College Station, TX 77843-3128 USA (e-mail: chang@ee.tamu.edu).

Digital Object Identifier 10.1109/TMTT.2005.864127

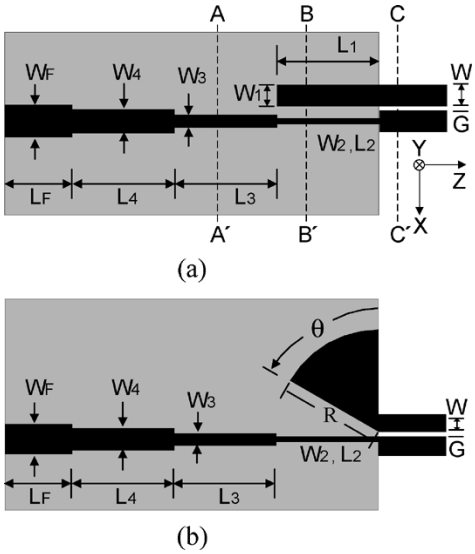

Fig. 1. Configurations of the microstrip-to-CPS transitions using: (a) rectangular open stub (type A) and (b) radial stub (type B).

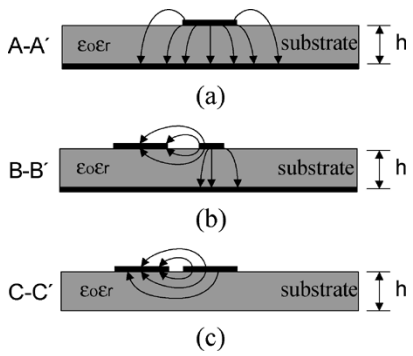

Fig. 2. Cross-sectional view of the electric distributions: (a) microstrip line, (b) coupled microstrip line, and (c) CPS.

is parallel to the y-axis and the electric field in the CPS is parallel to the x-axis, an electric-field rotation of 90° is needed. A quarter-wavelength rectangular open stub or a radial stub can be used for the field rotation. Fig. 2 shows the three cross-sectional views of the electric-field distributions at three locations shown in Fig. 1(a). The electric field changes from the microstrip-line mode $(A-A')$, through the transition mode $(B-B')$, to the CPS mode $(C-C')$. The electromagnetic-coupling-based transitions have the coupling region in the coupled microstrip-line mode region $(B - B')$. The quarter-wavelength rectangular open stub or the radial stub introduce the virtual short near the edge of the mode $B - B'$ and $C - C'$ regions at the center frequency. Since the virtual short is equal potential with the ground plane, some fields of the microstrip line couple to the edge of the virtual short, and the transition mode is formed. After the ground plane is removed, the CPS mode is obtained. In addition, since the characteristic impedance $(Z_{\rm cps})$ of the CPS is higher than 50 Ω of the microstrip line (Z_m), a multisection matching transformer is used. The transitions are all built on RT/Duroid 5870 substrates with a thickness $h = 0.508$ mm and a relative dielectric constant $\varepsilon_r = 2.33$. With the strip width $W = 1$ mm and gap $G = 0.2$ mm, the $Z_{\rm cps}$ is calculated as 155 Ω [11]. To match the 155 to 50 Ω, a Chebyshev three-section transformer (ripple level $\Gamma_m = 0.05$) with its sections' impedances of 124, 87, and 61 Ω is used [12] for the parametric study given in Section II-B.

B. Parametric Studies

In order to better understand this transition and derive some design guidelines, the shape of the stub, the angle of the radial stub, and the section number of the transformer are experimentally studied. First of all, as shown in Fig. 1, the two transitions with the rectangular open and radial stubs are investigated. The center frequency of the transition is designed at 7 GHz. The dimensions of the open and radial stubs are $L_1 = 7.6$ mm, $W_1 = 1$ mm, $R = 7.6$ mm, and $\theta = 80°$, where $L_1 = R = \lambda_g/4$, and λ_g is the guided wavelength at 7 GHz. A three-section impedance-matching transformer with its section impedances of 124, 87, and 61 Ω is used for impedance matching. The dimensions of the transitions are listed in Table I, shown as A1 and B1, where A1 denotes the transition using the rectangular stub and B1 denotes the one using the radial stub. For the convenience of measurement, the back-to-back transition with the microstrip-line input/output ports is used. Fig. 3 shows the measured results of the two transitions A1 and B1. The measured results are obtained by using network analyzer HP8510C with thru-reflect line (TRL) calibration to exclude the effects of the connectors and two 50-Ω microstrip lines. The insertion loss of the CPS are also excluded by measuring two pairs of back-to-back transitions with 10- and 20-mm-long CPSs. The insertion loss of a 10 –mm-long CPS could be estimated as the difference of the insertion loss of these two pairs of transitions. From 4.6 to 9.5 GHz, transition A1 shows a 3-dB insertion loss with the return loss of better than 10 dB. On the other hand, transition B1 has a return loss of better than 10 dB and an insertion loss of less than 3 dB from 4.6 to 10.5 GHz. The two transitions have a similar response at the center frequency band, while the major difference is near the upper bound of the bandwidth extends from 9.5 GHz of A1 to 10.5 GHz of B1. Since the impedance matching criteria are the same (i.e., same multisection impedance transformer), this suggests that the transition with the radial stub can provide a wider bandwidth due to the wide-band virtual short characteristic and the smoother field rotation by the radial stub in the coupling region.

Since the transition with radial stub can provide a wider bandwidth, the angles of the radial stub should also be investigated and optimized. Transitions with the radial stubs of different angles ($\theta = 80°$, 60°, and 40°) are compared. With the same three-section matching transformer, the transitions B1–B3 have their $\theta = 80°$, 60°, and 40° radial stubs, respectively. Fig. 4 shows the measured results. The 3-dB insertion-loss bandwidth of transition B1–B3 are 1.26–10.5 GHz, 1.37–9.8 GHz, and 1.52–9.5 GHz, respectively. This suggests that the transition with a 80° radial stub can provide a wider bandwidth. These three transitions have similar lower frequency band response. However, at high frequency, the effect of different angles is significant and the upper bound of the bandwidth extends from 9.5 GHz of B3 to 10.5 GHz of B1. For a good coupling, the gap between the microstrip line and radial stub should not be too big (compared with the guided wavelength). Otherwise, a little field couples to the CPS mode from the microstrip mode. This issue becomes even more serious when the frequency is higher and

TABLE I
DIMENSIONS OF THE TRANSITIONS (UNIT: MILLIMETERS)

Type A	W	G	W1	L1	W2	L2	W3	L3	W4	L4	WF	LF
A1	1	0.2	1	7.6	0.26	7.9	0.6	7.8	1.1	7.6	1.5	15

Type B	W	G	R	θ	W2	L2	W3	L3	W4	L4	WF	LF
B1	1	0.2	7.6	80	0.26	7.9	0.6	7.8	1.1	7.6	1.5	15
B2	1	0.2	7.6	60	0.26	7.9	0.6	7.8	1.1	7.6	1.5	15
B3	1	0.2	7.6	40	0.26	7.9	0.6	7.8	1.1	7.6	1.5	15
B4	1	0.2	7.6	60	0.6	7.6	N/A	N/A	N/A	N/A	1.5	15
B5	1	0.2	7.6	60	0.34	7.9	0.93	7.7	N/A	N/A	1.5	15
B6	1	0.2	7.6	80	0.22	4.3	0.38	7.9	0.66	7.8	1.5	10
	W5	L5	W6	L6								
	0.87	7.7	1.3	7.6								

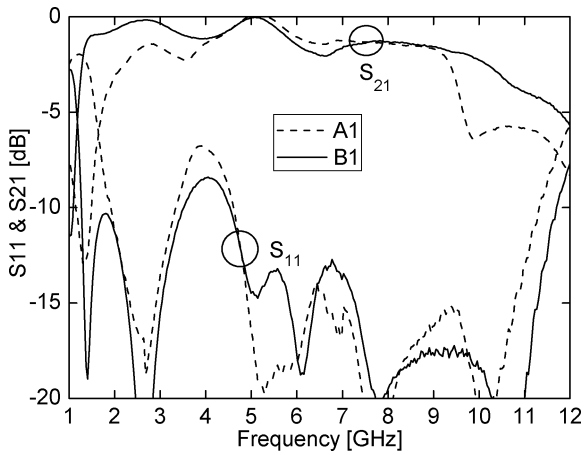

Fig. 3. Measured S-parameters for a back-to-back transition using rectangular stub (A1) and a back-to-back transition using radial stub (B1).

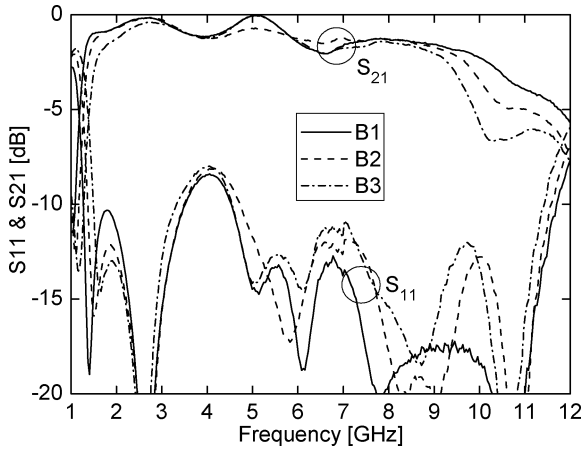

Fig. 4. Measured S-parameters of microstrip-to-CPS back-to-back transitions with $\theta = 80^\circ$ (B1), 60° (B2), and 40° (B3) radial stubs.

more electric field is confined between the microstrip line and the ground. The transition B1 has a 80° radial stub, and the gap between microstrip and the radial stub is smaller than the B2's and B3's. Therefore, the upper bound of the bandwidth extends from 9.5 GHz of B3 to 10.5 GHz of B1.

The bandwidth of the multisection matching transformer is determined by its section number [12] and, accordingly, the bandwidth of the transition will be determined by the multisection matching transformer. The transitions with the transformers

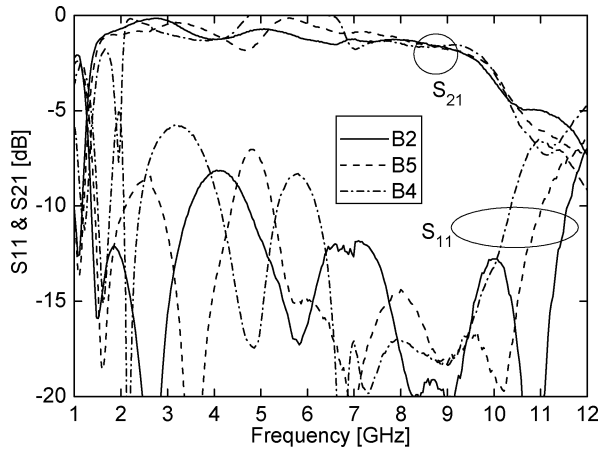

Fig. 5. Measured S-parameters of microstrip-to-CPS back-to-back transitions with three-section (B2), two-section (B5), and one-section (B4) matching transformers.

(ripple level $\Gamma_m = 0.05$) of different numbers of sections are studied. Fig. 5 shows the measured results. Transition B4 with one quarter-wavelength section (88 Ω) shows a return loss of better than 10 dB and an insertion loss of less than 3 dB from 6.2 to 10.2 GHz; transition B5 with two quarter-wavelength sections (112 and 68 Ω) shows a return loss of better than 10 dB and an insertion loss of less than 3 dB from 5.3 to 10 GHz; transition B2 with three quarter-wavelength sections (124, 87, and 61 Ω) shows a return loss of better than 10 dB and an insertion loss of less than 3 dB from 4.7 to 10.2 GHz. Since the coupling regions of these three transitions are very similar, the coupling mechanisms are similar. Therefore, impedance matching is critical in this case. As expected, the transition that uses a transformer with more sections can provide a wider bandwidth.

C. Optimal Design and Measurements

The transitions discussed in Section II-B are all designed based on transmission-line equations. They can help understand the transition; however, there are still parasitic effects and discontinuities that should be taken into consideration when these effects become more significant at high frequencies. For this purpose, a commercial full-wave electromagnetic simulator IE3D[1] is used to optimize the dimensions of transition B6 for the widest bandwidth. The five-section transformer of the ripple

[1]IE3D, ver. 10.1, Zeland Software Inc., Fremont, CA, 2003.

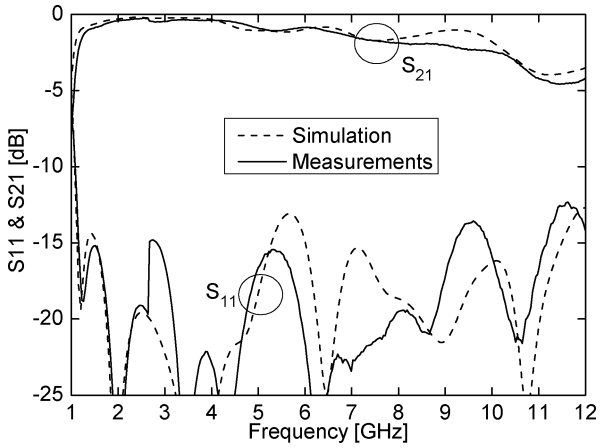

Fig. 6. Simulated and measured S-parameters of the optimal back-to-back microstrip-to-CPS transition B6.

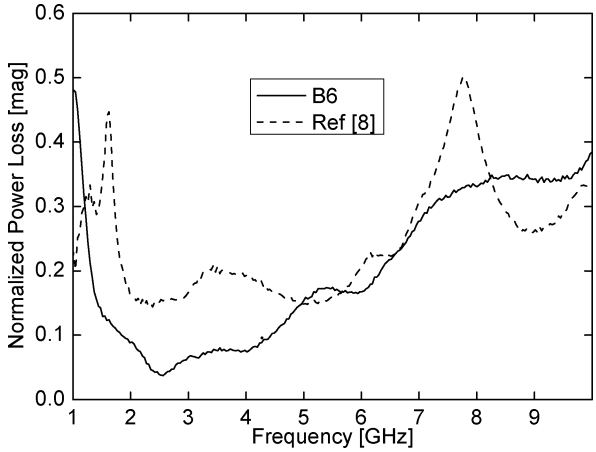

Fig. 7. Measured power loss of back-to-back optimal transition B6 and transition in [8].

level $\Gamma_m = 0.05$ is used for wide-band performance. Fig. 6 shows the simulated and measured results. With the measured return loss of better than 14 dB, the 1- and 3-dB back-to-back insertion loss bandwidth range from 1.4 to 6.6 GHz (1 : 4.7) and from 1.1 to 10.5 GHz (1 : 9.6), respectively. On the other hand, transition B1 only has a return loss better than 10 dB and an insertion of less than 3 dB from 4.6 to 10.5 GHz (1 : 2.3). With the aid of the full-wave simulator, the optimal transition B6 shows a much better performance than its prototype B1.

In summary, the design procedure is summarized as following.

1) Given the transition center frequency and substrate parameters, calculate the radius of the radial stub. The radius is $\lambda_g/4$, where λ_g is the guided wavelength at the center frequency.
2) Given the dimensions of CPS and required transition bandwidth, calculate $Z_{\rm cps}$ and determine the section number and each section's impedance of the multisection matching transformer.
3) With the initial parameters obtained from the above steps, using, for example, the full-wave electromagnetic simulator IE3D to take all parasitic effects into account and optimize the design.

Furthermore, it is interesting to observe that there are cutoff characteristics at the very low frequency end. Since the transitions are based on electromagnetic coupling (i.e., no dc connected), it is natural that these transitions have bandpass-like responses, where the passbands are located at the center frequency of the rectangular open stub/radial stub. The cutoff frequency depends on the bandwidths of the coupling stubs and multisection impedance transformer. The smaller bandwidth determines the total bandwidth of the transition. For example, if the coupling stubs have wider bandwidths, the bandwidth of the multisection transformer dominates the bandwidth of the transition (Fig. 5). Consequently, the low/high cutoff frequencies of the transition are dependent on the low/high cutoff frequencies of the transformer.

In addition, high power loss of a transition is undesired in high density circuits due to that it will cause unwanted crosstalk. Fig. 7 shows the normalized power loss of the optimal back-to-back transition B6 and the transition given in [8], where the normalized power loss is $1-|S_{11}|^2-|S_{21}|^2$. Since the transition in [8] uses taper ground and more power radiates out from the microstrip line, the power loss of B6 is smaller than that in [8] for most of the operation bandwidth, except at the 8.2–10-GHz band.

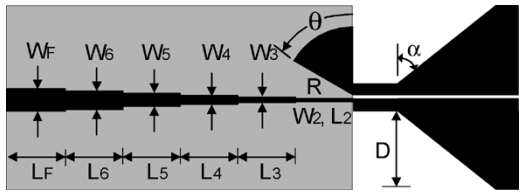

Fig. 8. Configuration of the microstrip-to-slotline transition ($\alpha = 60°$, $D = 9$ mm).

III. Microstrip-to—Slotline Transition Design and Measurement

Several microstrip line to slotline transitions have been reported [13]–[15]. Ideally, the double-Y balun in [13] and [14] has an all-pass response and no bandwidth limitation. However, due to the uncertainty in fabrication tolerance, it is difficult to keep all the stubs with the same impedance required in the design. In addition, the bandwidth is limited by imperfect stub terminations (open and short circuits), unequal dispersions between different transmission lines, and junction parasitics [16]. For Marchand baluns [15], the microstrip line and slotline are on different sides of the substrate. This double-side configuration requires two-side etching and alignment, which are more expensive and less accurate [17]. Uniplanar transitions are also reported [17], [18]. However, these transitions only show narrow-band performance.

The proposed uniplanar wide-band microstrip-to-CPS transition B6 developed in Section II is used as a building block for the microstrip-to-slotline transition design. Fig. 8 shows the configuration of the proposed microstrip-to-slotline transition. Since the gaps of the CPS and slotline are the same, the field matching is easily obtained. With the taper lines, the CPS of

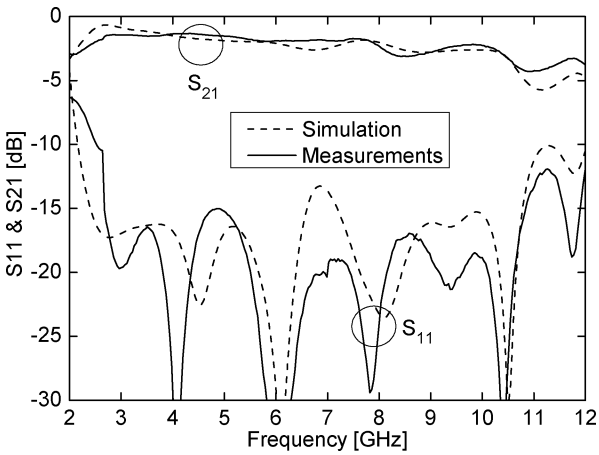

Fig. 9. Measured S-parameters of microstrip-to-slotline back-to-back transition.

155 Ω changes gradually into a slotline of 101 Ω, and the optimal taper angle α is found to be 60° by using IE3D. Fig. 9 shows the simulated and measured results. The measured results are obtained by using network analyzer HP8510C with TRL calibration to exclude the effects of the connectors and two 50-Ω microstrip lines. The insertion loss of the slotline are also excluded by measuring two pairs of back-to-back transitions with 10- and 20-mm-long slotlines. The insertion loss of a 10-mm-long slotline could be estimated as the difference of the insertion loss of these two pairs of transitions. From 2.7 to 10.4 GHz, the back-to-back return loss is better than 15 dB and insertion loss is less than 3 dB.

IV. Conclusions

In this paper, wide-band microstrip-to-CPS transitions have been proposed. Based on the transmission-line equations and experiment results, the design guidelines that can facilitate the optimization are derived. By using the commercial full-wave electromagnetic simulator IE3D, the optimal transition has a return loss of better than 14 dB, and the 1- and 3-dB back-to-back insertion loss are achieved from 1.4 to 6.6 GHz (1 : 4.7) and from 1.1 to 10.5 GHz (1 : 9.6), respectively. Furthermore, by tapering the CPS into a slotline, a wide-band microstrip-to-slotline transition has also been developed and has shown a return loss of better than 15 dB and a back-to-back insertion loss of less than 3 dB from 2.7 to 10.4 GHz (1 : 3.85). These wide-band uniplanar transitions on low dielectric-constant substrates should find numerous applications in antenna feeding networks and integrations with other devices.

Acknowledgment

The authors would like to thank M. Li, Texas A&M University, College Station, for his technical assistance and H. Li, Texas A&M University, College Station, for his helpful discussions.

References

[1] K. Goverdhanam, R. N. Simons, and L. P. B. Katehi, "Coplanar stripline components for high-frequency applications," *IEEE Trans. Microw. Theory Tech.*, vol. 45, no. 10, pp. 1725–1729, Oct. 1997.

[2] S.-G. Mao, H.-K. Chiou, and C. H. Chen, "Design and modeling of uniplanar double-balanced mixer," *IEEE Microw. Guided Wave Lett.*, vol. 8, no. 10, pp. 354–356, Oct. 1998.

[3] H.-T. Kim, S. Lee, S. Kim, Y. Kwon, and K.-S. Seo, "Millimeter-wave CPS distributed analogue MMIC phase shifter," *Electron. Lett.*, vol. 39, no. 23, pp. 1661–1662, Nov. 2003.

[4] L. Zhu and K. Wu, "Model-based characterization of CPS-fed printed dipole for innovative design of uniplanar integrated antenna," *IEEE Microw. Guided Wave Lett.*, vol. 9, no. 9, pp. 342–344, Sep. 1999.

[5] N. I. Dib, R. N. Simons, and L. P. B. Katehi, "New uniplanar transitions for circuit and antenna applications," *IEEE Trans. Microw. Theory Tech.*, vol. 43, no. 12, pp. 2868–2872, Dec. 1995.

[6] Y. Qian and T. Itoh, "A broad-band uniplanar microstrip-to-CPS transition," in *Proc. Asia–Pacific Microw. Conf.*, vol. 2, 1997, pp. 609–612.

[7] R. N. Simons, N. I. Dib, and L. P. B. Katehi, "Coplanar stripline to microstrip transition," *Electron. Lett.*, vol. 31, no. 20, pp. 1725–1726, Sep. 1995.

[8] Y.-H. Suh and K. Chang, "A wide-band coplanar stripline to microstrip transition," *IEEE Microw. Wireless Compon. Lett.*, vol. 11, no. 1, pp. 28–29, Jan. 2001.

[9] T. Chiu and Y.-S. Shen, "A broad-band transition between microstrip and coplanar stripline," *IEEE Microw. Wireless Compon. Lett.*, vol. 13, no. 2, pp. 66–68, Feb. 2003.

[10] J. S. Izadian and S. M. Izadian, *Microwave Transition Design*. Norwood, MA: Artech House, 1988, ch. 1.

[11] N. K. Das and D. M. Pozar, *PCAAMT—Personal Computer Aided Analysis of Multilayer Transmission Lines*. Amherst, MA: Univ. Massachusetts Press, Jun. 1990.

[12] D. M. Pozar, *Microwave Engineering*. New York: Wiley, 1998, ch. 5.

[13] V. Trifunovic and B. Jokanovic, "Review of printed Marchand and double Y baluns: Characteristics and applications," *IEEE Trans. Microw. Theory Tech.*, vol. 42, no. 8, pp. 1454–1462, Aug. 1994.

[14] B. Schtek and J. Kohler, "An improved microstrip-to-microslot transition," *IEEE Trans. Microw. Theory Tech.*, vol. MTT-23, no. 4, pp. 231–233, Apr. 1976.

[15] S. B. Cohn, "Slot line on a dielectric substrate," *IEEE Trans. Microw. Theory Tech.*, vol. MTT-17, no. 10, pp. 768–778, Oct. 1969.

[16] H. Gu and K. Wu, "Broadband design consideration of uniplanar double-Y baluns for hybrid and monolithic integrated circuits," in *IEEE MTT-S Int. Microw. Symp. Dig.*, 1999, pp. 863–866.

[17] N. I. Dib, R. N. Simons, and L. P. B. Katehi, "Broadband uniplanar microstrip to slot-line transitions," in *IEEE MTT-S Int. Microw. Symp. Dig.*, 1995, pp. 683–686.

[18] J. G. Yook, N. Dib, L. P. B. Katehi, R. N. Simons, and S. R. Taub, "Theoretical and experimental study of microstrip-to-slot line uniplanar transition," in *IEEE Int. Antennas Propag. Soc. Symp. Dig.*, 1994, pp. 1206–1209.

Wen-Hua Tu (S'04) received the B.S. degree in communication engineering from National Chiao Tung University, Hsinchu, Taiwan, R.O.C., in 1999, the M.S. degree in communication engineering from National Taiwan University, Taipei, Taiwan, R.O.C., in 2001, and is currently working toward the Ph.D. degree in electrical engineering at Texas A&M University, College Station.

Since 2003, he has been a Research Assistant with the Electromagnetics and Microwave Laboratory, Texas A&M University. His research interests include phased arrays and microwave devices and circuits.

Mr. Tu is a member of Phi Kappa Phi.

Kai Chang (S'75–M'76–SM'85–F'91) received the B.S.E.E. degree from the National Taiwan University, Taipei, Taiwan, R.O.C., in 1970, the M.S. degree from the State University of New York at Stony Brook, in 1972, and the Ph.D. degree from The University of Michigan at Ann Arbor, in 1976.

From 1972 to 1976, he was a Research Assistant with the Microwave Solid-State Circuits Group, Cooley Electronics Laboratory, The University of Michigan at Ann Arbor. From 1976 to 1978, he was with Shared Applications Inc., Ann Arbor, MI, where he was involved with computer simulation of microwave circuits and microwave tubes. From 1978 to 1981, he was with the Electron Dynamics Division, Hughes Aircraft Company, Torrance, CA, where he was involved in the research and development of millimeter-wave solid-state devices and circuits, power combiners, oscillators, and transmitters. From 1981 to 1985, he was with TRW Electronics and Defense, Redondo Beach, CA, as a Section Head, where he developed state-of-the-art millimeter-wave integrated circuits and subsystems including mixers, voltage-controlled oscillators (VCOs), transmitters, amplifiers, modulators, upconverters, switches, multipliers, receivers, and transceivers. In August 1985, he joined the Electrical Engineering Department, Texas A&M University, College Station, as an Associate Professor and became a Professor in 1988. In January 1990, he was appointed Raytheon E-Systems Endowed Professor of Electrical Engineering. He has authored and coauthored several books, including *Microwave Solid-State Circuits and Applications* (Wiley, 1994), *Microwave Ring Circuits and Antennas* (Wiley, 1996; 2nd edition 2004), *Integrated Active Antennas and Spatial Power Combining* (Wiley, 1996), *RF and Microwave Wireless Systems* (Wiley, 2000), and *RF and Microwave Circuit and Component Design for Wireless Systems* (Wiley, 2002). He has served as the Editor of the four-volume *Handbook of Microwave and Optical Components* (Wiley, 1989 and 1990; 2nd edition 2003). He is the Editor of *Microwave and Optical Technology Letters* and the Wiley Book Series on "Microwave and Optical Engineering" (over 70 books published). He has authored or coauthored over 450 papers and numerous book chapters in the areas of microwave and millimeter-wave devices, circuits, and antennas. He has graduated over 25 Ph.D. students and over 35 M.S. students. His current interests are microwave and millimeter-wave devices and circuits, microwave integrated circuits, integrated antennas, wide-band and active antennas, phased arrays, microwave power transmission, and microwave optical interactions.

Dr. Chang has served as technical committee member and session chair for the IEEE Microwave Theory and Techniques Society (IEEE MTT-S), the IEEE Antennas and Propagation Society (IEEE AP-S), and numerous international conferences. He was the vice general chair for the 2002 IEEE International Symposium on Antennas and Propagation. He was the recipient of the 1984 Special Achievement Award presented by TRW, the 1988 Halliburton Professor Award, the 1989 Distinguished Teaching Award, the 1992 Distinguished Research Award, and the 1996 Texas Engineering Experiment Station (TEES) Fellow Award presented by Texas A&M University.